Inorganica Chimica Acta, 29 (1978) 279–287

Photochemical and Kinetic Studies of Some Metal Dithizonate Complexes

CHRISTINE GEOSLING

Laser Physics Branch, Naval Research Laboratory, Washington, D.C. 20375, U.S.A.

ARTHUR W. ADAMSON*

Department of Chemistry, University of Southern California, Los Angeles, Calif. 9007, U.S.A.

ADOLFO R. GUTIERREZ

IBM Corporation K32/281, 5600 Cottle Rd., San Jose, Calif. 95193, U.S.A.

Received January 7, 1978

The kinetics of the approach to photostationary state have been studied for $Hg(HDz)_2$ in benzene and toluene, and for $Ag(HDz)$ in tetrahydrofuran, where HDz^- is the anion of dithizone (diphenylthiocarbazone). Photolysis converts the normal orange form to an unstable blue form which, while photointert, reverts thermally. Quantum yields are close to unity for 485 nm light, and from the photolysis kinetics, values of the first order thermal return rate constants, k, are obtained which agree well with the directly determined ones. The behavior of $Bi(HDz)_3$, $Pb(HDz)_2$, $Tl(HDz)$, $Cd(HDz)_2$, $Zn(HDz)_2$, $Cu(HDz)_2$, and $Pd(HDz)_2$ was also examined in various solvents. The return rates are fast and k values were obtained by means of laser pulse photolyses. The results allow for some differentiation between reaction schemes; it is concluded that for $Hg(HDz)_2$, both ligands isomerize following absorption of a light quantum by the complex. The k values for the set of complexes can be correlated approximately by type of solvent and type of central metal ion.

Introduction

Metal dithizonates form an interesting class of photochromic complexes. The most definitive study in the literature is that of Meriwether and co-workers [1], who reported on the preparation, the spectra, the qualitative photochemistry, and the thermal return rates for various dithizonates. Drawing on available crystallographic studies of the Hg(II) and Cu(II) complexes, on their visible and infrared absorption spectra for both the initial form and the photo-produced isomer in the case of the Hg(II) complex, and on the effect of deuteration on the return rate, they proposed the generic reaction shown in Fig. 1. Some additional literature is cited under Ref. 2.

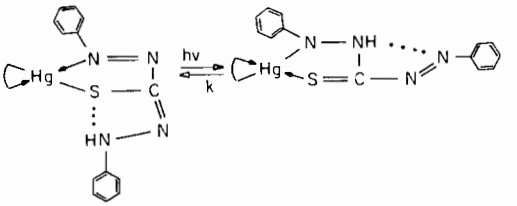

(1)

Figure 1. Probable structures of the orange and blue forms of $Hg(HDz)_2$.

The present study was undertaken for several reasons. First, we were interested in demonstrating experimentally the forward kinetics of approach to the photostationary state; Eq. (1) (Fig. 1) has speculative aspects and it was possible that complexities would appear in a quantitative study. Such a study would also yield the degree of conversion at the photostationary state and hence also the extinction coefficients of forms B and the quantum yields for the photoisomerization. In addition, the dithizonate complexes are well suited to pulse photolysis studies in that absorbances are high and the change in absorption spectrum large. We were interested in whether any indication could be found of delay in the formation of form B – delay that could be attributed either to unsuspected intermediates or to the decay time of the reacting excited state. Lastly, the pulse photolysis technique would allow determination of the rates of thermal return for the fast returning systems – none of which were known (except for an estimate in the case of Tl(HDz) [1]).

Experimental

Preparation of Dithizonate Complexes

The metal dithizonates were prepared by dissolving a salt of the corresponding metal, preferably the nitrate, in water adjusted to the appropriate pH [3, 4] and then rapidly adding (with stirring) the stoichiometric amount of purified dithizone [5]

*Address inquiries to this author.

TABLE I. Elemental Analyses and Properties of the Metal Dithizonates.

Compounds	M.p., °C		Elemental Analysis, % by wt.					
	Found	Reported[a]	Found[b]			Calculated		
			C	H	N	C	H	N
$Hg(HDz)_2$	228	228	43.97	3.32	15.67	43.91	3.12	15.76
$Ag(HDz)\cdot H_2O$	222	223	41.00	3.10	13.58	40.95	3.43	14.69
$Bi(HDz)_3$	216	219	49.04	3.46	17.16	48.04	3.41	17.24
$Bi(HDz)_2Cl\cdot 2HCl$	206	206–208	40.01	2.85	14.13	37.71	2.92	13.53
$Pb(HDz)_2$	247	246	43.85	3.02	15.44	43.49	3.08	15.61
Tl(HDz)	174	173–179						
$Cd(HDz)_2$	280	251–254	49.90	3.83		50.11	3.56	
$Zn(HDz)_2$	234	236–238	53.40	4.02	19.13	54.21	3.85	19.45
$Cu(HDz)_2$			52.95	3.63	18.95	54.38	3.86	19.51
$Pd(HDz)_2$	278	279	49.24	3.47	16.06	50.59	3.56	18.16

[a]Ref. 1. [b]Elek Microanalytical Laboratory, Los Angeles, Calif.

(diphenylthiocarbazone) in chloroform solution. The chloroform layer was separated and evaporated to dryness. The residue, consisting primarily of the desired product, was recrystallized from chloroform and vacuum dried at 80 °C for several hours. In the case of the mercury complex, recrystallization was from pyridine and then benzene; the silver dithizonate was recrystallized from distilled tetrahydrofuran (THF). Table I summarizes the melting point and analytical data.

Continuous Photolysis Experiments

Continuous photolysis runs were made with the mercury and silver dithizonates. The former was in dry benzene solution (except where otherwise noted), and the latter, in distilled, dry THF.

The irradiation arrangement was as follows. A Cary model 14R spectrophotometer was modified so as to accept a special sample holder in which a cell made from 1 cm square spectrophotometer tubing could be positioned. The bottom of the cell was rounded, to accomodate a stirring fin driven by a rotating magnet positioned below the cell. The sample holder was essentially a cylinder of axis at right angles to the light beam of the spectrophotometer, and fitted against an aperture drilled through the side of the Cary cell compartment. Filters could be mounted in the holder. The photolyzing light source was positioned just outside the Cary cell compartment, the irradiating light being filtered to the desired wavelength and impinging on the solution at right angles to the spectrophotometer beam. The irradiating source was a PEK high pressure mercury arc, and the interference filters selected light at 485 nm with a *ca.* 10 nm bandpass. There were also infrared and ultraviolet blocking filters present to ensure that minimal heating and u.v. decomposition occurred. The sample compartment could be thermostatted to a desired temperature by means of a connecting cryostat–thermostat bath, and the temperature of the solution being irradiated was monitored by means of a thermistor and appropriate measuring circuit.

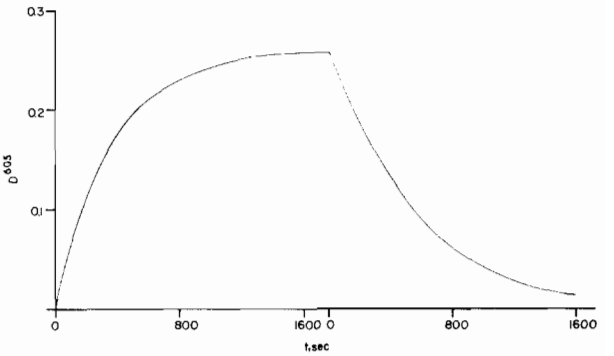

Figure 2. Typical spectrophotometer trace for the photolysis of $Hg(HDz)_2$ and its thermal return as monitored at 605 nm (data of Run 5 of Table II).

In a typical run, the solution of $Hg(HDz)_2$ was photolyzed at 485 nm, the wavelength region of the absorption maximum of form A, and the degree of isomerization to form B monitored by setting the Cary instrument for 605 nm. As illustrated in Figure 2, the chart recorder then showed increasing absorption as photolysis occurred and, upon blocking off the irradiating light, the dark return reaction as a decreasing absorbance.

Flash Photolysis Experiments

Flash photolysis was carried out with the use of an amplified and frequency doubled Q-switched Nd laser (Korad Co.) which produced up to 1.5 J. 20 nsec pulses at 530 nm. The frequency doubler was

a CD*A temperature tuned crystal. The usual range of pulse energy was 0.1 to 0.5 J, and the beam was collimated down to a diameter of 4–6 mm. The solution of dithizonate complex was in a 1 cm square 4-clear sided cell, with the monitoring beam at right angles to the photolyzing pulse. Monitoring was by means of a He/Ne laser or, where a different wavelength from 633 was desired, a suitably filtered, collimated beam from a d.c. Xe arc lamp (Hanovia).

An angled glass slide reflected a small portion of the exciting pulse onto a MgO surface which was seen by a fast photodiode (Korad model KD 1) of 0.5 nsec rise time, the signal from which controlled one beam of a Tektronix 7844 dual beam oscilloscope. The photolyzing pulse could thus be recorded with each experiment; calibrations of oscilloscope mV deflections *vs.* ballistic thermopile readings on the full beam provided a ±10% measure of the pulse energy. The monitoring beam was seen by an RCA 931B photomultiplier, preceded by an Oriel 724D grating monochromator, set to accept only the monitoring wavelength and, specifically, to screen out stray photolyzing and Raman scattered light. In some experiments, a 0.5 cm wide (monitoring beam path length) *vs.* 1 cm deep (photolyzing pulse pathlength) cell was used to minimize the depth of non-irradiated solution monitored. The output of the photomultiplier controlled the second beam of the oscilloscope. It was thus possible to photograph the trace showing either the rise time of product isomer absorption or, at longer sweep times, the decay of product absorption as thermal reaction returned the system to the starting form A. The oscilloscope deflection in mV was proportional to the monitoring beam intensity, so that the Beer–Lambert law for optical density at time t, D'_t, became $D'_t = \log (V_o/V_t)$, where the subscripts denote voltage for 100% transmission and at time t after the photolyzing pulse, and the voltages are referenced to zero V for zero light. For a first order thermal back reaction a plot of log D'_t *vs.* t should be linear for the usual case of zero absorption by form A at the monitoring wave length. The prime is used to distinguish optical density at a monitoring wave length from that at an irradiating wave length.

In the case of the $Pd(HDz)_2$ complex, it was more convenient to observe the return of absorption by form A following its bleaching by the photolyzing pulse. For a first order thermal back reaction, a plot of $\log[D'_\infty - D'_t]$ *vs.* t should be linear, where D'_∞ is the optical density to the monitoring beam at complete return (or before the photolyzing pulse).

Kinetic Treatment

Equation (1), while simple in statement, is complicated in its kinetic treatment because of the Beer's law term in the forward rate law. That is, it was highly convenient to monitor the degree of reaction by following the optical density near 605 nm,

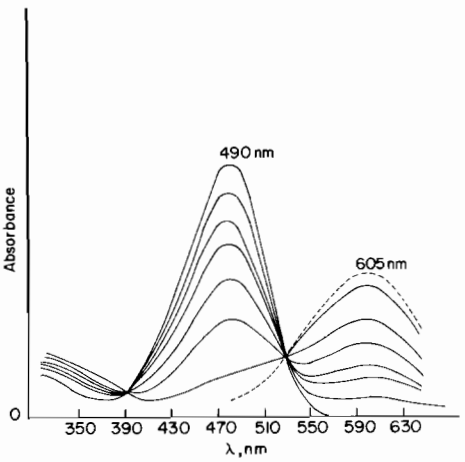

Figure 3. Spectral changes on photolysis (or on dark return) for $Hg(HDz)_2$ in benzene.

D′, a wavelength at which only form B absorbs in the cases of $Hg(HDz)_2$ and Ag(HDz). However, because the extinction coefficient for form B is less than that of form A, it was necessary to use solution concentrations such that the degree of absorption of photolyzing light by A was not linear in its concentration, (A). The net kinetic expression for d(B)/dt therefore required the full Beer's law formulation:

$$d(B)/dt = \phi I_o(1 - 10^{-D})(D_A/D) - k(B) \qquad (2)$$

Here, I_o is the incident light intensity in einsteins per sec per liter of solution being photolyzed, D is the total optical density at the irradiating wavelength, D_A is the optical density due to form A, again at the irradiating wavelength, ϕ is the quantum yield, and k is the rate constant for the dark return reaction. Since 1 cm square cells were used, the path length was 1 cm for both the photolyzing and the monitoring beam.

Equation (2) can be restated:

$$d[(B)/(A)^\circ]/dt = k[\alpha F - (B)/(A)^\circ] \qquad (3)$$

where $F = (1 - 10^{-D})(D_A/D)$, $\alpha = \phi I_o/k(A)^\circ$, and $(A)^\circ$ is the initial concentration of form A. At the photostationary state $d[(B)/(A)^\circ]/dt = 0$, so that $\alpha = (B)_{ss}/(A)^\circ F_{ss}$, the subscript ss denoting the steady state value. Equation (3) becomes

$$d[(B)/(B)_{ss}]/dt = k[F/F_{ss} - (B)/(B)_{ss}] \qquad (4)$$

Integration gives:

$$(B)/(B)_{ss} = k\int_o^t [F/F_{ss} - (B)/(B)_{ss}]\,dt \qquad (5)$$

or

$$D'/D'_{ss} = k\int_o^t [F/F_{ss} - D'/D'_{ss}]\,dt \qquad (6)$$

where D′ is optical density at the monitoring wavelength. From the change in absorption spectra with successive degrees of reaction, such as shown in Figure 3, D was found to be linear in D′. Thus in the kinetic studies, while D was not measured, it could

be calculated for each D′, and thus also F. The experimental test of the rate law was that the plot of D'/D'_{ss} *vs.* $\int^t [F/F_{ss} - D'/D'_{ss}]\,dt$ be linear over the course of the photolysis. Further, the slope of the plot gives k, and this value should be the same as that obtained by following the thermal return.

Evaluation of F was complicated by our inability to be certain of having obtained a solution which was 100% converted to the B form, and thus by our lack of independent knowledge of the extinction coefficient of B at the irradiating wavelength. Further, the preparative literature notes that dithizonates may contain similar absorbing, but photochemically inert components, possibly "secondary" dithizonates [1, 6]. It was not possible to rule out an impurity contribution of 10–15% to the optical density at the irradiating wavelength. Let D_i be the optical density due to impurity, and D°_B, that for pure form B at concentration (A)°. Then $D_A = D - D_i - D^\circ_B f_B$, where f_B is the degree of conversion of A to B. The same equation applies at the steady state, and manipulation gives

$$f_{A,ss} = (D_{ss} - a)/(D^\circ - a) \tag{7}$$

where $a = (D_i + D^\circ_B)$, f_A is the fraction of unisomerized A, and D° is initial optical density. Alternatively,

$$f_B = (D^\circ - D)/(D^\circ - a)$$
$$\text{and } f_{B,ss} = (D^\circ - D_{ss})/(D^\circ - a) \tag{8}$$

Thus the value of f_A and hence of D_A, needed in evaluating F, is dependent on the value of a (but not on D_i or D°_B separately):

$$D_A/D_{A,ss} = (D - a)/(D_{ss} - a) \tag{9}$$

Given *a*, F/F_{ss} follows, since D and D_{ss} are obtainable from the experimental D′ and D'_{ss} values (note that throughout D refers to optical density at the irradiating wavelength, and D′ to that at the monitoring wavelength).

In putting our photolysis data in the form of Eq. (6), there was thus a range of empirically allowed *a* values, namely between 0 and D_{ss}. Often this range was not large, as at lower temperatures where D_{ss} was about 0.1 of D°. Also, however, there was a small uncertainty in D'_{ss} (and hence in D_{ss}) in that a small residual drift upwards in D′ occurred after an apparent reaching of a stationary state. This was traced to slow mixing of a small fraction of the solution which tended to be trapped below the stirrer fins. However, only the terminal points were sensitive to this percent or two uncertainty. In optimizing the fit of data to Eq. (6), we computer searched for the best values of *a* and of D'_{ss}, each limited to its physically reasonable range. Some examples of the resulting plots are shown in Fig. 4. In general, the best fits gave k values from Eq. (6) which agreed well

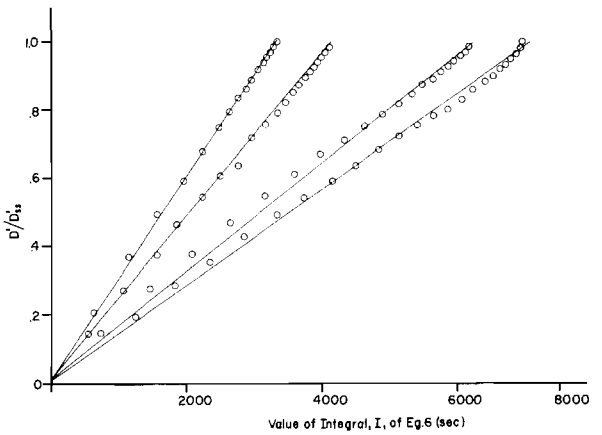

Figure 4. Photolysis of $Hg(HDz)_2$ in benzene plotting according to Eq. 6. These are for runs at various temperatures and provide an illustration of the fit to the kinetic analysis; the tendency for various samples to vary in their k value makes us discount the reliability of the activation energy implicit in this set of data.

with the directly determined ones from the thermal return reaction.

Calculation of ϕ required a knowledge of D°_A, and therefore of how *a* was partitioned between D_i and D°_B. That is,

$$\phi = \frac{(D^\circ - D_i)f_{B,ss}k}{\epsilon_A F_{ss} I_o} \tag{10}$$

where ϵ_A is the molar extinction coefficient of form A at the irradiating wavelength. The same was true in evaluating the concentration of B at any stage, and thus the extinction coefficient of B, that is,

$$\epsilon'_B = \frac{D'_{ss}\,\epsilon_A}{(D^\circ - D_i)f_{B,ss}}$$

For a given *a*, the choice of D_i determined D°_B and hence ϵ_B.

Results

Continuous Photolysis Experiments

Spectra of photolyzed solutions of $Hg(HDz)_2$

A typical spectral sequence for successive degrees of photolysis of $Hg(HDz)_2$ in benzene is shown in Fig. 3. Isosbestic points were well maintained, indicating that no secondary photolysis or reaction products formed. The extinction coefficient of the initial orange form A is reported to be 7.0×10^4 M^{-1} cm^{-1} at the absorption maximum of 490 nm [1]; our value is 6.9×19^4 M^{-1} cm^{-1}. The extinction coefficient of the product blue isomer B could be inferred from the detailed kinetic studies (Table II)

TABLE II. Continuous Photolysis of Dithizonate Complexes at 485 nm.

Run	Complex[a]	Solvent	Temp. °C	Fitting Parameters		Calculated Parameters			Thermal Return
				$f_{B,ss}$	a/D°	ϕ[b]	$10^{-4}\,\epsilon'_B$ M^{-1} cm^{-1}	10^3k sec^{-1}	10^3 k sec^{-1}
1.	$Hg(HDz)_2$	benzene	24	0.80	0.21	.95	2.8	0.53	0.53
2.	$Hg(HDz)_2$	benzene	24	0.84	0.32	1.04	2.6	0.49	0.48
3.	$Hg(HDz)_2$[c]	benzene[a]	25	0.94	0.18	.85	2.7	1.08	1.07
4.	$Hg(Hdz)_2$[c]	benzene[a]	25	0.95	0.16	.88	2.9	1.24	1.23
5.	$Hg(HDz)_2$	benzene	45	0.53	0.30	.73	2.6	1.81	1.81
6.	$Hg(HDz)_2$	toluene	15	0.90	0.24	1.00	2.5	0.41	0.41
7.	$Hg(HDz)_2$[d]	toluene	15	0.76	0.44	1.05	2.2	0.45	0.45
8.	$Hg(HDz)_2$[c]	benzene[e]	15	0.94	0.14	.95	2.2	0.96	0.95
9.	Ag(HDz)	THF	2–3	0.35	0.70	1.08	0.75	3.14	3.13

[a]Concentrations varied about 10^{-5} *M*. just before use; $D_i/D°$ taken to be zero. [b]Assuming $D_i/D° = 1/3\ a/D°$ unless otherwise indicated. [c]Solution chromatographed [d]415 nm irradiation. [e]Water saturated.

to be $2.7 \times 10^4\ M^{-1}$ cm^{-1} at 605 nm. Preliminary to such studies we determined that B was not itself photosensitive; the rate of its thermal return to A was not influenced by incident light at the absorption maximum of 605 nm.

Photolysis kinetics of $Hg(HDz)_2$

The details of the algebraic procedures are given under Experimental. The best fitting parameters for several of the runs are given in Table II. The principal observation is that the data indeed fit the kinetic treatment and that the values of k obtained from the photolysis agreed well with those determined by following the thermal back reaction. Additional points are the following. It is seen that the $a/D°$ values range from 0.21 to 0.32. Some limits can be inferred for the partitioning of a between D_i and $D°_B$. First, it is unlikely that $D_i/D°$ exceeded 0.1 in view of the agreement of our ϵ_A with literature. Second, with low temperature runs such as that shown in Fig. 4, the degree of conversion at the photostationary state was large enough to infer that $D°_B/D°$ was less than about 0.2. The observed $a/D°$ values are thus acceptable, and the values for ϕ and ϵ'_B in the table are calculated assuming that each best fitting $a/D°$ should be partitioned 1/3 $D_i/D°$ and 2/3 $D°_B/D°$. We find $\phi = 0.9 \pm 0.1$, $\epsilon'_B = 2.7 \times 10^4\ M^{-1}$ cm^{-1} (605 nm) as compared to $3.9_1 \times 10^4\ M^{-1}$ cm^{-1} (in Ref. 1), and $\epsilon_B = 1.0 \times 10^4\ M^{-1}$ cm^{-1} (485 nm).

Additional observations were the following. If the benzene solution of $Hg(HDz)_2$ was chromatographed through alumina prior to use, $a/D°$ values of 0.16–0.18 resulted; these lower figures suggest that indeed a $D_i/D°$ contribution of about 0.1 was present in the other runs. Saturation of the benzene with water results in only small changes in the parameters. These data did not obey Eq. (6) well, however, suggesting that some new complexity was present in the kinetics. Two runs were made in dry toluene, one using 415 nm irradiating light. Only small changes in parameters were found.

Continuous photolysis of Ag(HDz)

The same procedures were used as for the mercury complex, the same irradiation wavelength, and the same algebraic treatment of data. Photoproduct absorption was monitored at its band maximum of 595 nm, however, Again, D was obtained from D′ using a correlation plot obtained from the sequence of spectra as thermal return occurred. For solubility reasons, it was necessary to change solvent to tetrahydrofuran (THF). Return rates were faster than for $Hg(HDz)_2$ and the runs were limited to 2–3 °C. The forward photolyses obeyed Eq. (6) well, and results for one of the runs are included in Table II. The quantum yield was essentially unity; note the large value of $a/D°$.

Thermal Return Rates; Pulse Photolysis Studies

$Hg(HDz)_2$

The extinction coefficient of form A is negligible at the monitoring wavelength of 605 nm and plots of logD′ *vs.* t were linear, as expected for a first order reaction. Several such plots are shown in Fig. 5. A previous report [1] that the thermal return rate constant was dependent on total $Hg(HDz)_2$ concentration could not be confirmed. At *ca.* 20 °C we found 10^4 k values to be 1.98, 1.79, 1.80, and 1.91 sec^{-1} for concentrations of 2.8, 2.2, 1.7, and 1.1 ($\times 10^{-5}$), respectively. On the other hand, the return rates while always accurately first order, were not reproducible from one preparation to the next. Also, there was some dependence on the exact cleaning

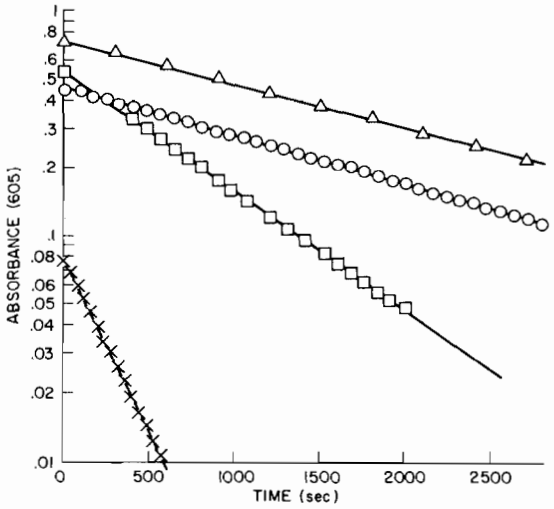

Figure 5. First order plot of thermal return reactions for Hg(HDz)$_2$ and Ag(HDz) in benzene. △, Hg(HDz) at 20 °C; ○, Hg(HDz)$_2$ Run 2; □, Hg(HDz)$_2$ Run 4; ×, Ag (HDz), Run 9. Run numbers refer to Table II.

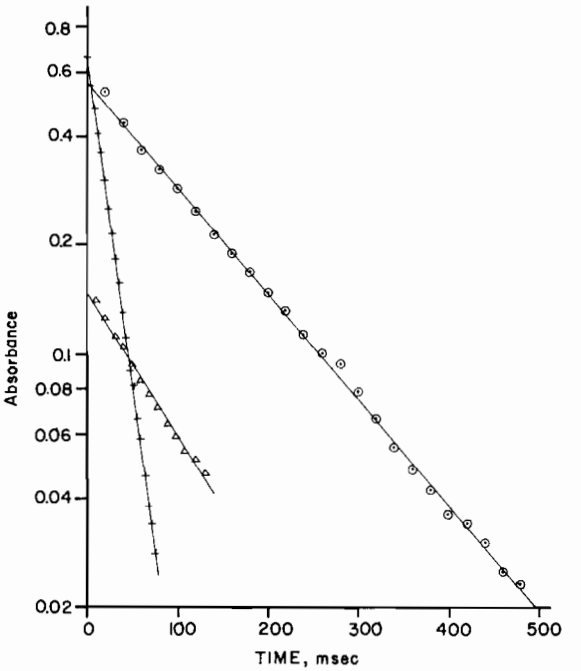

Figure 6. First order plots of thermal return reactions for various dithizonate complexes. ○, Pb(HDz)$_2$, Run 3; +, Hg(HDz)$_2$, Run 7; △, Zn(HDz)$_2$, Run 10. Run numbers refer to Table III.

treatment of the glassware. This complexity in the thermal return mechanism prevents us from reporting any reliable activation energies.

Pulse photolysis monitoring studies

In the cases of Hg(HDz)$_2$ in benzene and of Ag(HDz) in THF, we looked for possible delay in the appearance of photoproduct. That is, the change in monitoring beam intensity during and immediately after the photolyzing pulse was examined for evidence of delayed appearance of product, as might occur if it derived from an excited state of a few nsec or longer lifetime, or if some intermediate were formed. No such effect was detected; the transmitted intensity of the monitoring beam changed from the initial value to that for the product in close parallel to the integrated laser pulse. We conclude that in both cases the reactive excited state lifetime is less than 10 nsec. Nor was there any evidence for excited state absorption, or for transient chemical intermediates.

Thermal return rates following pulse photolysis

A number of experiments were performed in which the thermal return rate was followed by monitoring changes in optical density following a photolyzing pulse. Several transcriptions of the oscilloscope photographs are shown in Fig. 6. In all cases the return was first order within experimental error and over at least two halflives. The results are summarized in Table III. The temperatures varied somewhat as all were determined by the ambient temperature. The solvents chosen were generally the least polar in which the complex was adequately soluble. Certain solvents were ruled out because of evident decomposition or reaction of the complex. This was true for Pb(HDz)$_2$ in THF, which reacted to change from a red to a yellow solution. In three systems, the effect of changing solvent was determined: Cd(HDz)$_2$, Hg(HDz)$_2$, and Zn(HDz)$_2$. Cu(HDz)$_2$ changed sufficiently rapidly in acetone solution that only the first photolysis of a fresh solution was reliable. While some temperature dependence is implicit in the various data, because of the mechanistic uncertainty with Hg(HDz)$_2$, we report no activation energies for other dithizonates.

Discussion

Photolysis and Thermal Return Kinetics

All of the systems studied here were photochromic, including one, that of Cu(HDz)$_2$, not previously so reported. As noted by Meriwether, Breitner, and Sloan (MBS) [1]. The type of reaction seems to be uniform; in all but one case, photolysis shifts a strong absorption band at about 500 nm to a somewhat weaker one at about 600 nm. Qualitatively, the type of reaction is: Orange form $\underset{k}{\overset{h\nu}{\rightleftarrows}}$ Blue form. An exception is Pd(HDz)$_2$, for which the initial form has an additional absorption at 635 nm and a color change of green to pink in non-polar solvents. With this

TABLE III. Thermal Return Rates Following Pulse Photolysis[a].

No.	nm	Compound	Solvent	Temp. °C	Absorption Spectrum		Thermal Return	
					$10^4 \epsilon$ M^{-1} cm^{-1}	λ_{max}[b] nm	half-life msec	k sec^{-1}
1	633	$Bi(HDz)_3$	CH_2Cl_2	27.7	7.5	492 (498)	335 ± 17	2.0
2	633	$Bi(HDz)_2Cl{\cdot}2HCl$	CH_2Cl_2	26	3.2 .67	503 (500) 607 (620)	370 ± 10	1.9
3	633	$Pb(HDz)_2$	CH_2Cl_2	*Ca.* 25	6.5	513 (520) (608sh)	110 ± 7	6.5
4	633	Tl(HDz)	Benzene	*Ca.* 25	2.3 2.3	390 502 (518, 605sh)	18 ± 2	38
5[c]	605	$Hg(HDz)_2$	Benzene	24	7.0	490	1.4×10^3[d]	5.0×10^{-4}
6[c]	605		Toluene	15	7.0	490	1.61×10^3[d]	4.3×10^{-4}
7	633		Ethanol	26	7.0	490	76 ± 5	9.1
8	633	$Cd(HDz)_2$	THF	28	8.3	503 (518, 605sh)	308 ± 16	2.3
9	633		Acetone	26			8.0 ± 0.8	86 ± 10
10	633	$Zn(HDz)_2$	THF	28			16 ± 1	43
11[e]			CH_2Cl_2	21	8.2	530 (532)	9.5×10^3 ± 400	0.073
12	633	$Ag(HDz){\cdot}H_2O$	THF	29	3.7	465 (470)	2.7×10^3 ± 100	0.26
13[f]	597	$Cu(HDz)_2$	Acetone	26	1.1 0.88	420 (445) 525	96	7.2
14[g]	630	$Pd(HDz)_2$	CH_2Cl_2	26	3.7 3.2	498 635	150	4.6

[a]Excitation was at 530 nm, and monitoring for disappearance of photo-product as noted. [b]Values in parenthesis are from Ref. 1. [c]Data from Table II. [d]Half-life in sec. [e]Return followed by ordinary spectrophotometry. [f]More than one form is reported [1]; our preparation was black or dark brown. Half-life is for fresh solution as slow irreversible decomposition occurred. [g]More than one form is reported [1]; our preparation was violet, but solutions were green.

exception, the visible band is evidently ligand centered with little metal–ligand field or metal–ligand charge transfer character. A corollary is that the O and B configurations are essentially the same for the whole series.

With respect to literature comparisons of our results, we agree generally with the visible absorption spectra reported by MBS; the differences (Table III) are probably not significant. No quantum yields seem to have been reported previously with which to compare our values for $Hg(HDz)_2$ and Ag(HDz). We can, however, compare our thermal return rates for these two complexes with those of Meriwether, Breitner, and Colthup (MBC) [1]. For the $Hg(HDz)_2$ complex our k value of about 0.5×10^{-3} at 24 °C is distinctly lower than that of 2.7×10^{-3} reported by MBC for 25 °C. We do not find as large an effect of water and find no effect of complex concentration on k. We suspect that active and inactive B forms may exist in equilibrium and that the thermal return may be subject to dust and other surface catalysis.

For Ag(HDz) in THF we find k to be 0.017 sec^{-1} at 11.5 °C (by interpolation); MBC report 0.011 sec^{-1}, in fair agreement. MBS quote a preliminary half-life for Tl(HDz) in benzene at 25 °C of about 30 msec; we find 18 msec at 29 °C.

We turn next to the nature of the kinetic scheme for the photochromism. All of the thermal return reactions were first order and, in the cases of $Hg(HDz)_2$ and Ag(HDz), the photochemical forward reaction was also first order (in intensity of light absorbed by the O form; that is, after allowing for the Beer's law correction). These observations leave several possibilities, however. We frame these in terms of a $M(HDz)_2$ species.

Scheme (1)

The two ligands are assumed to be fully independent, each contributing additively to light absorption and exhibiting independent photochemistry and thermal kinetics. In this scheme, $\phi_1 = \phi_2$,

$$\text{O–M–O} \underset{k_2}{\overset{h\nu,\phi_1}{\rightleftharpoons}} \text{O–M–B} \underset{k_1}{\overset{h\nu,\phi_2}{\rightleftharpoons}} \text{B–M–B}, \qquad (12)$$

$k_1 = 2k_2$ on statistical grounds, and $\epsilon_{O\text{–}M\text{–}O} = 2\epsilon_O$, $\epsilon_{O\text{–}M\text{–}B} = \epsilon_O + \epsilon_B$, and $\epsilon_{B\text{–}M\text{–}B} = 2\epsilon_B$ where ϵ_O and ϵ_B are the independent extinction coefficients for the O and B forms of a given complexed ligand.

This scheme fits our thermal rate law; the return rate is given by $D'/D'_{ss} = \exp(-k_2 t)$ and so is first order. Also, Eq. (6) would fit the approach to stationary state of a system obeying this scheme.

We rule out the scheme on several grounds, however. Consider first the photochemical sequence. Two quanta minimum are required to convert O–M–O to B–M–B, whereas in Table II, our yields are close to unity. That is, a ϕ of unity as calculated by means of Eq. (10) means that one mol of O–Hg–O is converted to B–Hg–B by one einstein of light, or two ligands per quantum (similar, less precise values could be obtained from initial photolysis rates; that is, our yields are obtainable independently of the algebra of Eq. (6)). We thus can rule out O–M–B as an intermediate, photolysis of which is required to produce B–M–B.

A qualitative ground for discarding scheme (1) is that it seems improbable that ϕ_2 would be comparable to ϕ_1 were an O–M–B species a photochemical intermediate. Absorption of a light quantum by O–M–B would produce O*–M–B, and one would expect efficient intramolecular energy transfer to give O–M–B*, since, judging from the absorption spectra, the B form has a lower lying state than the orange form. Since coordinated B is not photoreactive, the effect would be to make ϕ_2 small were the sequence of Eq. (12) in fact present.

If we thus conclude that the forward photolysis leads directly to B–M–B, we now find a difficulty with the thermal sequence of scheme (1). The minimum possible value for D_{ss}/D_o is 1/3 since at the photostationary state, (O–M–B) must be twice (B–M–B) if $k_1 = 2k_2$. At the lower temperatures, values of D_{ss}/D_o as low as 0.1 were observed in the case of $Hg(HDz)_2$, or well below this minimum value. Thus the statistical model cannot be correct for the thermal return process.

We can also rule out moderate deviations from this model. On photolyzing to nearly complete conversion to B–Hg–B, and then allowing thermal return to occur, the concentration of O–Hg–B should be at a maximum after about two thermal return half-lives if a nearly statistical model applied (in the pure statistical model, there would be 25% B–Hg–B, 50% O–Hg–B, and 25% O–Hg–O, or 50% conversion of B to O). If now, photolysis is *resumed,* a curve of approach to stationary state should be observed that would not superimpose on the corresponding section of the original photolysis curve (at the lower temperatures, and assuming the pure statistical model, at 50% O → B conversion, the system would consist essentially of 50% O–Hg–O and 50% B–Hg–B, and thus be of a distinctly different composition). No such deviation was found.

The statistical thermal return scheme can perhaps be discounted on a qualitative ground as well. In view of the pronounced dependence of the thermal return rate on the nature of M (Table III), it seems unlikely that the B → O conversion of one ligand would transmit no influence on the probability of the B → O conversion of the second one.

Scheme (2)

We abandon O–M–B as a relatively stable intermediate and now have four related possibilities:

$$\text{O–M–O} \xrightarrow{h\nu,\phi} \underset{k}{\overset{}{\text{O–M–B}}} \xrightarrow{\text{fast}} \text{B–M–B} \qquad (13)$$

$$\text{O–M–O} \xleftarrow[\text{fast}]{} \underset{\text{O–M–B}}{\overset{h\nu,\phi}{\longrightarrow}} \xleftarrow[k]{} \text{B–M–B} \qquad (14)$$

$$\text{O–M–O} \underset{k}{\overset{h\nu,\phi}{\rightleftharpoons}} \text{B–M–B} \qquad (15)$$

$$\text{O–M–O} \xleftarrow[k]{} \underset{\text{O–M–B}}{\overset{h\nu,\phi}{\longrightarrow}} \underset{\text{K(rapid)}}{\rightleftharpoons} \text{B–M–B} \qquad (16)$$

In Eq. (13), photolysis produces chemical intermediate O–M–B which decays rapidly to B–M–B, while the return is concerted (we cannot have both the photolysis and the thermal return going through the same unstable intermediate). We consider Eq. (13) unlikely on the grounds that in none of the pulse photolysis experiments was any evidence observed for a transient species (if $k_{\text{O–M–B}\rightarrow\text{B–M–B}} > 10^8$ sec^{-1}, then, of course, (13) is possible).

In Eqs. (14) and (15), the photolytic conversion is concerted and the thermal return is either through an unstable O–M–B, or is concerted. In Eq. (16), O–M–B is in rapid equilibrium with B–M–B, and the O–M–B → O–M–O process is rate limiting. Any of these versions would fit our rate observations and the quantum yield data for $Hg(HDz)_2$, but Eq. (16) could not apply to Ag(HDz) or Tl(HDz).

We conclude at this point that at least for $Hg(HDz)_2$, both ligands isomerize essentially simultaneously, following light absorption. The coordination geometry is that of a highly distorted tetrahedron or, alternatively a linear S–Hg–S configuration is distorted by weak Hg–N bonds [7]. The shift in metal–ligand bond polarities that probably occurs on excitation probably also changes the coordination geometry and could well dispose both ligands toward isomerization. The high quantum yields and the lack of delay in appearance of photoproducts indicate a very prompt excited state reaction.

Thermal Return Rate Correlations

The pulse photolysis results provide a range of thermal return rate constants not before available, and it is of interest to examine the set for trends. Figure 7 displays the results, classed by solvent. The data of Tables II and III are used directly, except that the values ofr $Zn(HDz)_2$ in THF and for Hg-

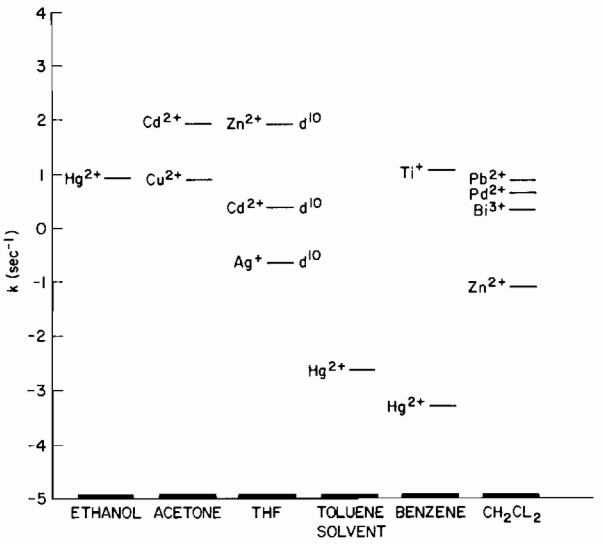

Figure 7. Solvent dependence of thermal return rate constants for dithizonate complexes at *ca.* 27 °C.

$(HDz)_2$ in toluene are corrected to 27 °C assuming a reasonable activation energy for a tautomerism of this type (25 kcal/mol).

In addition to the clear solvent dependence, the log k values vary with periodic table row (Zn *vs.* Cd) and with electron configuration. Comparison of $Pb(HDz)_2$ and $Bi(HDz)_3$ suggests that the effect of oxidation number is small, perhaps a reasonable conclusion since in each case the molecule is neutral in overall charge. More detailed analysis seems unwarranted because of the uncertainty of the detailed thermal return reaction mechanism. Qualitatively, however, the solvent effects seem not to correlate with simple rating schemes, such as the Hildebrand solubility parameter [8], or Gutmann's donor numbers [9]. There is partial correlation with solvent "Z" values [10]. Also, the dependence of log k on M shows some qualitative correlation with hard–soft concepts [11], log k decreasing with increasing "softness" of M, but not with the more quantitative hard–soft scales [12, 13].

Acknowledgement

These investigations were supported by National Science Foundation Grant CHE 74-08535 and Office of Naval Research Contract N00014-76-C-0548, both with the University of South California.

References

1 L. S. Meriwether, E. C. Breitner, and C. L. Sloan, *J. Am. Chem. Soc., 87,* 4441 (1965); L. S. Meriwether, E. C. Breitner, and N. B. Colthup, *ibid., 87,* 4448 (1965).
2 (a) J. L. A. Webb, I. S. Bhatia, A. H. Corwin, and A. G. Sharp, *J. Am. Chem. Soc., 72,* 91 (1950). (b) G. Venturello and A. M. Ghe, *Anal. Chim. Acta, 45,* 1054 (1955). (c) H. M. N. H. Irving and R. S. Ramakrishna, *J. Chem. Soc.,* 2118 (1961). (d) V. R. Schmidt and R. Rautschke, *Acta Histochem., 15,* 359 (1963). (e) G. B. Briscoe and B. C. Cooksey, *J. Chem. Soc.,* 205 (1969). (f) H. M. N. H. Irving, A. M. Nabelsi, and S. Sahota, *Anal. Chim. Acta, 67,* 135 (1973) and earlier papers. (g) Von Urs P. Wild, *Chimia, 27,* 421 (1973). (h) A. C. Fabretti and G. Payonel, *J. Inorg. Nuclear Chem., 37, 603 (1975). (i) M.* Kryszewski, B. Nadolski, and A. Fabrycy, *Roczn. Chem., 49,* 2077 (1975).
3 H. Freiser, *Chemist Analyst., 50,* 62 (1961).
4 E. B. Sandell, "Colorimetric Determination of Trace Metals," Interscience, New York (1959).
5 J. H. Billman and E. S. Cleland, *J. Am. Chem. Soc., 65,* 1300 (1943).
6 T. Nowicka-Jankowska and H. M. N. H. Irving, *Anal. Chim. Acta, 54,* 489 (1971).
7 M. M. Harding, *J. Chem. Soc.,* 4136 (1958).
8 J. H. Hildebrand and R. L. Scott, "The Solubility of Non-Electrolytes", 3rd ed., Dover Publications, New York (1964).
9 V. Gutmann, "Coordination Chemistry in Non-Aqueous Solutions", Springer-Verlag, Vienna (1968) (and references therein), and V. Gutmann, *Coord. Chem. Rev., 12, 263 (1974).*
10 V. Gutmann, *Coord. Chem. Rev., 18,* 225 (1976) and references therein.
11 R. G. Pearson, *J. Am. Chem. Soc., 85,* 3533 (1963) and related papers.
12 A. Yinst and D. A. McDaniel, *Inorg. Chem., 6,* 1067 (1967).
13 M. Misono and Y. Saito, *Bull. Chem. Soc. Japan, 43,* 3680 (1976).